J|A|C|S
ARTICLES
Published on Web 05/16/2006

Four Tautomers of Isolated Guanine from Infrared Laser Spectroscopy in Helium Nanodroplets

Myong Yong Choi* and Roger E. Miller†

Contribution from the Department of Chemistry, The University of North Carolina, Chapel Hill, North Carolina 27599

Received February 9, 2006; E-mail: mychois@unc.edu

Abstract: Infrared laser spectroscopy is used to study the four lowest energy tautomers of guanine, isolated in helium nanodroplets. The large number of vibrational bands observed in the infrared spectrum are assigned by comparing the corresponding experimental vibrational transition moment angles with those obtained from ab initio theory. The result is the conclusive assignment of the spectrum to the N9H-Keto, N7H-Keto, N9Ha-Enol(trans), and N9Hb-Enol(cis) tautomers. The dipole moments of these tautomers are also experimentally determined and compared with ab initio theory.

I. Introduction

Nucleic acid bases (NABs) are of fundamental importance in biology, forming the building blocks for the genetic code for life.[1] Their various tautomers have been shown to play a central role in mutation.[2] In recent years, there has been growing interest in characterizing the isolated systems so that detailed comparisons can be made between theory and experiment. To date, however, the theoretical studies of these systems have far outpaced the experiments. Nevertheless, there are a growing number of experimental methods that provide at least some information on these important systems, in particular using microwave[3−7] and IR−UV laser[8,9] spectroscopic methods. An interesting aspect of many NABs, including guanine, is the existence of various conformers, and a number of gas-phase studies have been directed at identifying these structures and determining their relative energies.[10−13]

Studies of this type require that the molecule be vaporized, so that gas-phase spectroscopy can be used. Although many of these systems are thermally stable, making vaporization by simple thermal evaporation possible, guanine has proven to be somewhat more challenging. Indeed, Nir et al.[14] have recently stated that "Especially guanine cannot be vaporized intactly by simple thermal heating." For this reason, considerable effort has been expended by several groups to make use of laser desorption methods,[14−16] which suffer less from thermal decomposition.[17−19]

Because of its thermal instability, guanine is the only NAB for which microwave spectra have not been reported.[20] As a result, the experimental identification of the tautomers of guanine has been attempted exclusively by infrared laser spectroscopy.[8,14,15,21−23] It is interesting to note that even microwave spectroscopy, often considered the most definitive gas-phase structural probe, can have difficulties in distinguishing between the various tautomers for NABs, as we previously demonstrated for cytosine.[24] The gas-phase infrared studies from a number of different laboratories have also produced conflicting structural assignments. Specifically, Mons et al.[15] and Nir et al.[8,14] have both used IR−UV depletion spectroscopy to study the tautomers of guanine, with conflicting results. Figure 1 shows the various tautomers of guanine, which differ in the location of the hydrogen atom attached to the nitrogen atom in position 7 or 9, in their keto and enol forms. In addition, the enol forms have two rotational orientations of the OH group,

† Deceased November 6, 2005.

(1) Weinkauf, R.; Schermann, J. P.; de Vries, M. S.; Kleinermanns, K. *Eur. Phys. J. D* **2002**, *20*, 309−316.
(2) Podolyan, Y.; Gorb, L.; Leszczynski, J. *Int. J. Mol. Sci.* **2003**, *4*, 410−421.
(3) Brown, R. D.; Godfrey, P. D.; Mcnaughton, D.; Pierlot, A. P. *J. Am. Chem. Soc.* **1988**, *110*, 2329−2330.
(4) Brown, R. D.; Godfrey, P. D.; Mcnaughton, D.; Pierlot, A. P. *J. Chem. Soc., Chem. Commun.* **1989**, *1*, 37−38.
(5) Brown, R. D.; Godfrey, P. D.; McNaughton, D.; Pierlot, A. P. *Chem. Phys. Lett.* **1989**, *156*, 61−63.
(6) Brown, R. D.; Godfrey, P. D.; McNaughton, D.; Pierlot, A. P. *J. Am. Chem. Soc.* **1989**, *111*, 2308−2310.
(7) Godfrey, P. D.; Brown, R. D. *J. Am. Chem. Soc.* **1995**, *117*, 2019−2023.
(8) Nir, E.; Janzen, Ch.; Imhof, P.; Kleinermanns, K.; de Vries, M. S. *J. Chem. Phys.* **2001**, *115*, 4604−4611.
(9) Plutzer, Ch.; Hunig, I.; Kleinermanns, K. *Phys. Chem. Chem. Phys.* **2003**, *5*, 1158−1163.
(10) Robertson, E. G.; Simons, J. P. *Phys. Chem. Chem. Phys.* **2001**, *3*, 1−18.
(11) Nir, E.; Janzen, Ch.; Imhof, P.; Kleinermanns, K.; de Vries, M. S. *Phys. Chem. Chem. Phys.* **2002**, *4*, 740−750.
(12) Bienko, D. C.; Michalska, D.; Roszak, S.; Wojciechowski, W.; Nowak, M. J.; Lapinski, L. *J. Phys. Chem. A* **1997**, *101*, 7834−7841.
(13) McCarthy, W.; Smets, J.; Adamowicz, L.; Plokhotnichenko, A. M.; Radchenko, E. D.; Sheina, G. G.; Stepanian, S. G. *Mol. Phys.* **1997**, *91*, 513−525.
(14) Nir, E.; Plützer, Ch.; Kleinermanns, K.; de Vries, M. *Eur. Phys. J. D* **2002**, *20*, 317−329.
(15) Mons, M.; Dimicoli, I.; Piuzzi, F.; Tardivel, B.; Elhanine, M. *J. Phys. Chem. A* **2002**, *106*, 5088−5094.
(16) Brauer, B.; Gerber, R. B.; Kabeláč, M.; Hobza, P.; Bakker, J. M.; Abo-Riziq, A. G.; de Vries, M. S. *J. Phys. Chem. A* **2005**, *109*, 6974−6984.
(17) Junk, G.; Svec, H. *J. Am. Chem. Soc.* **1963**, *85*, 839−845.
(18) Gaffney, J. S.; Pierce, R. C.; Friedman, L. *J. Am. Chem. Soc.* **1977**, *99*, 4293−4298.
(19) Basiuk, V. A.; Navarro-González, R. *Icarus* **1998**, *134*, 269−278.
(20) Nir, E.; Grace, L.; Brauer, B.; de Vries, M. S. *J. Am. Chem. Soc.* **1999**, *121*, 4896−4897.
(21) Szczepaniak, K.; Szczesniak, M. *J. Mol. Struct.* **1987**, *156*, 29−42.
(22) Sheina, G. G.; Stepanian, S. G.; Radchenko, E. D.; Blagoi, Yu. P. *J. Mol. Struct.* **1987**, *158*, 275−292.
(23) Crews, B.; Abo-Riziq, A.; Grace, L.; Callahan, M.; Kabeláč, M.; Hobza, P.; de Vries, M. S. *Phys. Chem. Chem. Phys.* **2005**, *7*, 3015−3020.
(24) Choi, M. Y.; Dong, F.; Miller, R. E. *Philos. Trans. R. Soc. A* **2005**, *363*, 393−413.

10.1021/ja060741l CCC: $33.50

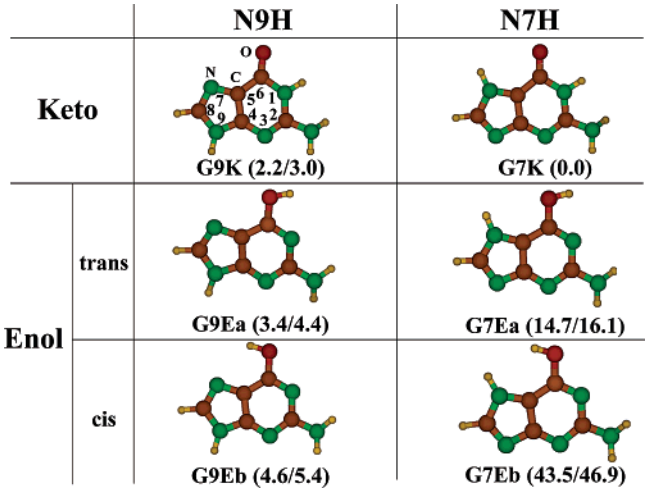

Figure 1. Ab initio structures and relative energies (MP2/aug-cc-pVDZ level) of the various tautomers of guanine. Amino-oxo (keto) and amino-hydroxy (enol) are classified by certain functional groups in the positions 2 and 6 of the purine base, namely NH_2 (amino-), C═O (-oxo), and O−H (-hydroxy). In addition, the enol forms have two rotational orientation of the OH group: trans (a-form) and cis (b-form) to the five-membered ring. The values in parentheses give the energies relative to G7K in kilojoules per mole with/without a harmonic zero-point energy correction. Only the four lowest energy tautomers are experimentally observed in the present study.

which are designated as a and b. Because the naming schemes are not the same, we have introduced a third nomenclature, which is somewhat more systematic than the other two. Nir et al.[8,14] observed spectral features which they assigned to the G9K, G7K, and G9Ea tautomers, whose structures are shown in Figure 1. In contrast, Mons et al.[15] reported the observation of four isomers, corresponding to structures of G9K, G7K, G9E(a or b), and G7Ea in Figure 1. The disagreement with regard to the assignments of the observed tautomers has not been resolved to date.

The primary reason for the discrepancy between the various assignments is that the vibrational frequencies of the various tautomers are rather similar, making it difficult to unambiguously assign the structures simply by comparison between the experimental and ab initio vibrational frequencies. We have recently introduced a new approach for assigning such vibrational spectra, based upon comparisons between the vibrational transition moment angles (VTMAs)[25] determined from theory and experiment. These VTMAs are defined as the angle between the transition moment for a particular vibrational mode and the permanent electric dipole moment. The experimental measurement of these angles requires that the molecule be oriented in the laboratory frame of reference, which is done using a large direct current (dc) electric field. This pendular-state spectroscopy has been discussed in detail in the literature.[26−29]

We have found that, for high-frequency H−X stretching vibrational modes, the VTMAs are quantitatively determined by modest ab initio calculations.[25] Unlike the vibrational frequency calculations, no scaling factor is required for the comparison between experiment and theory. In this paper we apply this method to the study of the various tautomers of guanine. We obtain conclusive assignment of the infrared spectra (3400−3650 cm^{-1} region) of the guanine tautomers as a result of comparisons of the experimental vibrational frequencies, VTMAs, and dipole moments with those obtained from high-level ab initio calculations.

II. Experimental Method

The infrared spectra of isolated guanine were obtained using a helium nanodroplet apparatus that has been described in detail previously.[30] Helium nanodroplets were formed by expanding ultrahigh-purity helium (99.9999%) in a vacuum through a 5 μm diameter orifice. The spectra were recorded using a source pressure of 55 atm, the nozzle being maintained at 21 K by use of a closed-cycle helium refrigerator. Under these conditions, droplets are produced with a mean size of approximately 3000 helium atoms. The droplets were doped with guanine from the gas phase, using a heated oven. Although there have been a number of failed attempts at evaporating guanine,[8,14,15] due to thermal decomposition of the sample, we observed no such effects at the oven temperature of 350 °C used here. The present success is most likely the result of the fact that helium nanodroplet experiments require much lower vapor pressures than those typically used in free-jet experiments.[31] For all of the experiments discussed here, the oven temperature was adjusted so that the only significant features in the corresponding spectra are attributable to the guanine monomer.

The seeded droplets pass between two parallel gold-coated mirrors, where they are irradiated by multiple passes of a continuous-wave tunable infrared laser (a PPLN-OPO laser[32,33]). Upon vibrational excitation of the solvated molecules, vibrational relaxation to the helium results in the evaporation of several hundred helium atoms from each droplet. Detection is then based on the depletion of the helium beam flux in the forward direction, using a bolometer detector.[34] In practice, the laser was amplitude modulated, and the signals were recorded using phase-sensitive detection.

A large dc electric field was applied to the laser interaction region using two electrodes positioned at right angles to the multipass cell. The laser electric field was aligned either parallel or perpendicular to the dc electric field. The signal levels associated with a given vibrational band could then be recorded as a function of the electric field strength and polarization direction. This was necessary in order to measure the associated VTMAs. At the low temperatures characteristic of both free-jet expansions[27,35−38] and helium nanodroplets,[39−42] a polar molecule can be strongly oriented along the dc electric field direction. For such an oriented molecule, the infrared transition intensity depends on the direction (relative to the permanent dipole direction) and magnitude of both the vibrational transition moment and the laser electric field. In the present study, the vibrational bands were recorded at zero electric field and at high fields (80 kV/cm) corresponding to parallel and

(25) Dong, F.; Miller, R. E. *Science* **2002**, *298*, 1227−1230.
(26) Rost, J. M.; Griffin, J. C.; Friedrich, B.; Herschbach, D. R. *Phys. Rev. Lett.* **1992**, *68*, 1299−1301.
(27) Block, P. A.; Bohac, E. J.; Miller, R. E. *Phys. Rev. Lett.* **1992**, *68*, 1303−1306.
(28) Friedrich, B.; Herschbach, D. *Int. Rev. Phys. Chem.* **1996**, *15*, 325−344.
(29) Friedrich, B.; Herschbach, D. R. *Nature* **1991**, *353*, 412−414.
(30) Nauta, K.; Miller, R. E. *J. Chem. Phys.* **1999**, *111*, 3426−3433.
(31) Lindinger, A.; Toennies, J. P.; Vilesov, A. F. *J. Chem. Phys.* **1999**, *110*, 1429−1436.
(32) Schneider, K.; Kramper, P.; Schiller, S.; Mlynek, J. *Opt. Lett.* **1997**, *22*, 1293−1295.
(33) Schneider, K.; Kramper, P.; Mor, O.; Schiller, S.; Mlynek, J. *Advanced Solid State Lasers*; Trends in Optics and Photonics 19; Optical Society of America: Washington, DC, 1998; pp 256−258.
(34) Gough, T. E.; Miller, R. E.; Scoles, G. *Appl. Phys. Lett.* **1977**, *30*, 338−340.
(35) Fraser, G. T.; Pine, A. S.; Lafferty, W. J.; Miller, R. E. *J. Chem. Phys.* **1987**, *87*, 1502−1508.
(36) Wu, M.; Bemish, R. J.; Miller, R. E. *J. Chem. Phys.* **1994**, *101*, 9447−9456.
(37) Bemish, R. J.; Chan, M. C.; Miller, R. E. *Chem. Phys. Lett.* **1996**, *251*, 182−188.
(38) Moore, D. T.; Oudejans, L.; Miller, R. E. *J. Chem. Phys.* **1999**, *110*, 197−208.
(39) Nauta, K.; Miller, R. E. *Science* **1999**, *283*, 1895−1897.
(40) Nauta, K.; Miller, R. E. *Phys. Rev. Lett.* **1999**, *82*, 4480−4483.
(41) Miller, R. E. *SPIE Proc.* **1998**, *3271*, 151−163.
(42) Nauta, K.; Moore, D. T.; Stiles, P. L.; Miller, R. E. *Science* **2001**, *292*, 481−484.

perpendicular laser polarization directions (relative to the dc field). The approach is quite analogous to that of linear dichroism in bulk phases.[43]

Vibrational Transition Moment Angles (VTMAs). The permanent dipole orientation distribution for a polar molecule in a dc electric field can be calculated accurately using the methods discussed most thoroughly by Kong and co-workers.[44−46] Given that the present vibrational spectra are not rotationally resolved, the dipole orientation distributions, $P(\cos\theta)$, represent a thermal average over the Stark levels at the rotational temperature of the molecules in the droplets (0.37 K[47]). This distribution is given by

$$P(\cos\theta) = \int_0^{2\pi} P(\cos(\theta,\varphi))\,\mathrm{d}\varphi = {}^1/_2(1 + \sum_{n=1}^{\infty} a_n P_n(\cos\theta)) \quad (1)$$

where

$$a_n = (n + 1/2)\sum_M N_M \sum_\tau \mathrm{e}^{-E_{\tau M}/k_B T} \sum_{J_1,J_2,K,s_1,s_2} C^{\tau M}_{J_1 K s_1} C^{\tau M}_{J_2 K s_2} [1 + (-1)^{s_1+s_2+J_1+J_2+n}](-1)^{M-K} N_K \times \frac{[(2J_1+1)(2J_2+1)]^{1/2}}{2} \begin{pmatrix} J_2 & J_1 & n \\ M & -M & 0 \end{pmatrix} \begin{pmatrix} J_2 & J_1 & n \\ K & -K & 0 \end{pmatrix} \quad (2)$$

$$\begin{pmatrix} J_2 & J_1 & n \\ M & -M & 0 \end{pmatrix} \text{is a 3-}J\text{ symbol,}$$

N_M is the degeneracy for each M value, and N_K is the nuclear statistical weight. It is important to note that the Stark energies in this equation depend on both the dipole moment of the molecule and its rotational constants. However, the thermal average is only weakly dependent upon these quantities, so that we can use the ab initio values (the rotational constants being reduced by a factor of 3 to account for the effects of the helium[48]) in this analysis.

With the molecule oriented in the laboratory frame of reference, the vibrational band intensity depends on the angle α, defined as the angle between the permanent electric dipole and the transition moment (the VTMA). For a vibrational mode with its transition moment parallel to the permanent moment, and therefore also the dc electric field, the intensity of the associated band is enhanced by the application of a dc field when the laser electric field is aligned parallel to the dc field. Rotation of the laser polarization by 90° will result in a field-induced decrease in the corresponding band intensity, because in this case the laser is polarized perpendicular to the transition moment. At the magic angle (54.7°), the intensity of the band will not depend on the electric field.[49] Throughout this paper, parallel and perpendicular polarization configurations correspond to the laser being polarized parallel and perpendicular to the dc electric field, respectively. The parallel and perpendicular band intensities can now be written in terms of both α and the permanent dipole distribution:

$$A_{\parallel}(\alpha) = \int_0^{2\pi}\mathrm{d}\varphi \int_0^{2\pi}\mathrm{d}\chi \int_0^{\pi} P(\cos\theta)[\sin\theta\cos\chi\sin\alpha - \cos\theta\cos\alpha]^2 \sin\theta\,\mathrm{d}\theta \quad (3)$$

$$A_{\perp}(\alpha) = \int_0^{2\pi}\mathrm{d}\varphi \int_0^{2\pi}\mathrm{d}\chi \int_0^{\pi} P(\cos\theta)[\cos\varphi\cos\theta\cos\chi\sin\alpha - \sin\varphi\sin\chi\sin\alpha - \cos\varphi\sin\theta\cos\alpha]^2 \sin\theta\,\mathrm{d}\theta \quad (4)$$

As a result, the ratio of the intensities corresponding to parallel and perpendicular polarization is given by

$$\rho(\alpha) = \frac{A_{\parallel}(\alpha)}{A_{\perp}(\alpha)} = \frac{2\int_0^{\pi} P(\cos\theta)[2\cos^2\theta + \sin^2\alpha - 3\cos^2\theta\sin^2\alpha]\sin\theta\,\mathrm{d}\theta}{\int_0^{\pi} P(\cos\theta)[2 - \sin^2\alpha - 2\cos^2\theta + 3\cos^2\theta\sin^2\alpha]\sin\theta\,\mathrm{d}\theta} \quad (5)$$

The experimental intensity ratios are obtained by integrating the area under the vibrational bands (with parallel and perpendicular polarization configurations), using the corresponding field-free spectra to normalize. The latter is necessary given that a different laser alignment was needed for the two measurements and one could not rely on the optimizations alone to ensure that the overall pumping efficiency was the same for both. The VTMAs for the various vibrational modes of the molecule were then determined by comparing the calculated intensity ratios with those obtained from eq 5.

Ab Initio Calculations. The ab initio VTMAs, obtained by full geometry optimization and harmonic vibrational analysis using Gaussian 03,[50] were carried out using Møller−Plesset perturbation theory at the second-order level (MP2) with a 6-311++G(d,p) basis set and an aug-cc-pVDZ basis set. Figure 1 shows the lowest six tautomers of guanine, with relative energies listed in kilojoules per mole, with and without zero-point energy corrections. In both cases, the amino-oxo G7K tautomer has the lowest energy. In general, the free energy is more useful for comparison with experiment, particularly given that guanine is produced at a temperature of 350 °C in the oven. Rapid quenching of the guanine upon capture by a helium droplet is likely to freeze in the corresponding tautomer population distribution,[24,51−56] making the free energy at the oven temperature the most relevant quantity. Figure 2 shows a plot of the calculated free energies for the lowest four tautomers of guanine. The vertical dashed line corresponds to the experimental conditions used here. According to this measure, the G7K tautomer is the most stable tautomer, which agrees generally with the energy ordering of the various tautomers.[57] Nevertheless, all four of these have sufficiently low free energies in comparison to the temperature of the oven that we would expect to see them all. In contrast, the next-lowest form lies approximately 15 kJ/mol higher in free energy and therefore is unlikely to be present in our samples. The relative intensities of these four taumomers will be discussed below.

Figure 3 shows the four lowest energy tautomers of guanine, onto which are superimposed vectors representing the directions of the permanent electric dipole moments (solid arrows) and the vibrational transition moments (dashed arrows). The magnitudes of the various moments are given in Table 1. It is clear from the figure that the patterns of VTMAs for the various tautomers are quite different, making them a useful tool for assigning the associated vibrational spectra.

It is interesting to note that the permanent electric dipole moments are quite different for the four tautomers shown in Figure 3, namely

(43) Holmen, A. *J. Phys. Chem. A* **1997**, *101*, 4361−4374.
(44) Kong, W.; Bulthuis, J. *J. Phys. Chem. A* **2000**, *104*, 1055−1063.
(45) Kong, W. *Int. J. Mod. Phys. B* **2001**, *15*, 3471−3502.
(46) Franks, K. J.; Li, H. Z.; Kong, W. *J. Chem. Phys.* **1999**, *110*, 11779−11788.
(47) Hartmann, M.; Miller, R. E.; Toennies, J. P.; Vilesov, A. F. *Phys. Rev. Lett.* **1995**, *75*, 1566−1569.
(48) Callegari, C.; Lehmann, K. K.; Schmied, R.; Scoles, G. *J. Chem. Phys.* **2001**, *115*, 10090−10110.
(49) Michl, J.; Thulstrup, E. W. *Spectroscopy with polarized light: solute alignment by photoselection, in liquid crystals, polymers, and membranes*; VCH Publisher Inc.: Weinheim, 1995.
(50) Frisch, M. J.; et al. *Gaussian 03*, Revision C.02; Gaussian, Inc.: Wallingford, CT, 2004.
(51) Potts, A. R.; Baer, T. *J. Phys. Chem. A* **1997**, *101*, 8970−8978.
(52) Potts, A. R.; Baer, T. *J. Chem. Phys.* **1996**, *105*, 7605−7612.
(53) Potts, A. R.; Baer, T. *J. Chem. Phys.* **1998**, *108*, 869−875.
(54) Reva, I. D.; Stepanian, S. G.; Adamowicz, L.; Fausto, R. *Chem. Phys. Lett.* **2003**, *374*, 631−638.
(55) Pettersson, M.; Macoas, E. M. S.; Khriachtchev, L.; Fausto, R.; Rasanen, M. *J. Am. Chem. Soc.* **2003**, *125*, 4058−4059.
(56) Choi, M. Y.; Miller, R. E. *Phys. Chem. Chem. Phys.* **2005**, *7*, 3565−3573.
(57) Hanus, M.; Ryjáček, F.; Kabeláč, M.; Kubař, T.; Bogdan, T. V.; Trygubenko, S. A.; Hobza, P. *J. Am. Chem. Soc.* **2003**, *125*, 7678−7688.

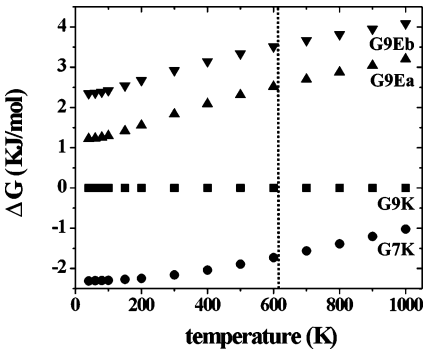

Figure 2. Ab initio free energies for the four lowest energy tautomers of guanine as a function of temperature. The vertical dashed line corresponds to the experimental conditions used here at 620 K.

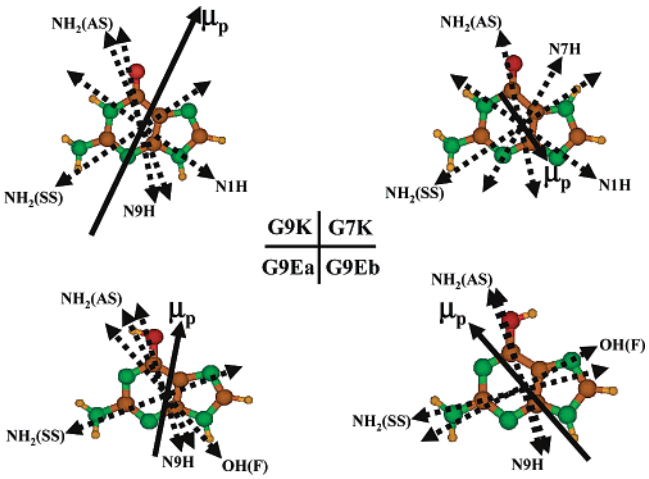

Figure 3. The four lowest energy tautomers of guanine, showing the corresponding directions of the permanent electric dipole moments (the length of the solid arrow is proportional to the dipole magnitudes) and the vibrational transition moments (dashed arrows) for the various vibrational modes. The magnitudes of these moments are given in Table 1.

6.26, 1.88, 3.11, and 4.06 D for tautomers G9K, G7K, G9Ea, and G9Eb, respectively. Given that the experimentally measured dipole moments for molecules solvated in helium are only slightly different from the corresponding gas-phase values,[58] these can also be used to help in the spectral assignments, as discussed below.

III. Results

The upper panel in Figure 4 shows an experimental spectrum of guanine in helium that spans the regions corresponding to the N−H, NH_2, and O−H stretching vibrations. The other four panels show the ab initio spectra (all scaled by a factor of 0.957 with a 6-311++G(d,p) basis set) for the four lowest energy tautomers of guanine. Unlike the IR-REMPI method used by a large number of groups,[8,10,15,59,60] the present method does not separate out the contributions to the spectrum associated with the different tautomers. Rather, this linear spectroscopy shows all of the bands in a single spectrum. The apparent difficulty with this is that there are many bands that are closely spaced, making an assignment based purely on the vibrational frequencies impossible. This problem is compounded by the fact that the accuracy of scaled ab initio calculations is less than the spacing between the various bands. Note, for example, that there is a large discrepancy between the experimental and scaled ab initio frequencies for the two free O−H stretching bands of the G9Ea and G9Eb isomers. As we will see below, the group of bands in the experimental spectrum, near 3575 cm^{-1}, includes these O−H stretches. Even if a pump−probe method were used to separate out the spectra for the different tautomers, a unique assignment could not be made, given that some of the vibrational frequencies do not depend very strongly on the tautomer geometry. We believe that this is, in part, the reason for the differences in the assignments for the various experimental studies.

In an effort to overcome the problem discussed above, we now turn to the measurement of the VTMAs for the various bands in the experimental spectrum. Figure 5 shows an expanded view of the highest frequency cluster of bands near 3585 cm^{-1} measured with (a) parallel polarization, (b) zero electric field, and (c) perpendicular polarization (the corresponding electric field being 80 kV/cm). Given that these bands do not correspond at all to the scaled ab initio calculations, an assignment based upon frequencies would be pure guesswork. However, qualitatively it seems reasonable that these four bands correspond to the O−H and NH_2 asymmetric stretches of the G9Ea and G9Eb tautomers, which are the only ones that are anywhere close to this region. This would imply that the O−H stretches are much lower in frequency than predicted by the scaled ab initio results, a fact that has been noted in previous studies,[24,56] while the asymmetric NH_2 stretches are higher than those from theory. Stated differently, the empirical scaling factors for the various vibrational modes are different, making the ab initio frequencies of limited use.

It is clear from Figure 5 that two of the bands are enhanced in intensity by application of an electric field with parallel polarization, while the other two are enhanced with perpendicular polarization, one more strongly (iii) than the other (iv). Quantitative analysis of the data reveals that these two bands have experimental VTMAs of (iii) 85° and (iv) 65°. This is to be compared with the ab initio VTMAs for the O−H stretches of the G9Ea and G9Eb tautomers of 83° and 57°, respectively. Bands (i) and (ii) were similarly analyzed to give experimental VTMAs of 38° and 22°, respectively. Here again, the agreement with ab initio theory is excellent, the corresponding values for the G9Ea and G9Eb tautomers being 37° and 20° for the asymmetric NH_2 bands. The ability to uniquely assign the spectra of these rotamers has a great deal of potential for obtaining a more quantitative understanding of the intramolecular interactions between various functional groups in such systems. Indeed, it is interesting to note that the experimental O−H stretch (3584.4 cm^{-1}) for the G9Ea tautomer is lower in frequency than the corresponding vibration for the G9Eb tautomer (3590.6 cm^{-1}). This ordering and frequency difference (6.2 cm^{-1}) is in excellent agreement with the ab initio calculations (6.6 cm^{-1}), even though the absolute scaled frequencies are not as well reproduced. Such differences are most likely reflective of the difference in the intramolecular interactions in the cis and trans configurations. The same is true for the asymmetric NH_2 stretches, where again the ordering and frequency differences for the cis and trans tautomers are consistent between theory and experiment. It is worth pointing out here that the ability to resolve the spectra associated with

(58) Stiles, P. L.; Nauta, K.; Miller, R. E. *Phys. Rev. Lett.* **2003**, *90*, 135301−4.
(59) Zwier, T. S. *J. Phys. Chem. A* **2001**, *105*, 8827−8839.
(60) Plützer, Ch.; Nir, E.; de Vries, M. S.; Kleinermanns, K. *Phys. Chem. Chem. Phys.* **2001**, *3*, 5466−5469.

Table 1. Experimental and ab Initio Vibrational Data for the Guanine Tautomers

tautomer	harmonic frequency[a] (cm^{-1})	scaled frequency[a] (cm^{-1})	exptl frequency (cm^{-1})	IR intensity (km/mol)	assignment	ab initio VTMAs[b] (°)	exptl VTMAs (°)	dipole (D)
G9K	3701.3	3542.2	3544.5	38.7	NH_2 (AS)	44	50	6.26
	3664.8	3507.2	3506.9	100.4	N9H	42	44	
	3606.6	3451.5	3437.9	58.8	N1H	80[77]	68	
	3587.7	3433.4	3444.5	44.7	NH_2 (SS)	31	40	
G7K	3687.1	3528.6	3526.6	36.7	NH_2 (AS)	29	29	1.88
	3660.6	3503.2	3504.8	120.2	N7H	73	73	
	3607.4	3452.3	3441.1	64.3	N1H	47[41]	20	
	3576.2	3422.4	3430.5	38.1	NH_2 (SS)	83	80	
G9Ea	3801.1	3637.6	3584.4	109.6	OH (F)	57	65	3.11
	3737.9	3577.2	3580.9	41.5	NH_2 (AS)	37	38	
	3669.6	3511.8	3511.3	104.0	N9H	34	33	
	3610.6	3455.3	3465.2	58.1	NH_2 (SS)	60	55	
G9Eb	3807.9	3644.2	3590.6	100.3	OH (F)	83	85	4.06
	3741.7	3580.8	3583.2	45.3	NH_2 (AS)	20	22	
	3667.4	3509.7	3509.6	105.1	N9H	21	18	
	3612.3	3457.0	3466.1	66.2	NH_2 (SS)	73	73	

[a] The ab initio calculations were performed at the MP2/6-311++G(d,p) level, and the scaled frequencies were obtained by multiplying the harmonic frequencies by a factor of 0.957. [b] The ab initio VTMAs for the NIH bands presented in square brackets were obtained at the MP2 level of theory with an aug-cc-pVDZ basis set.

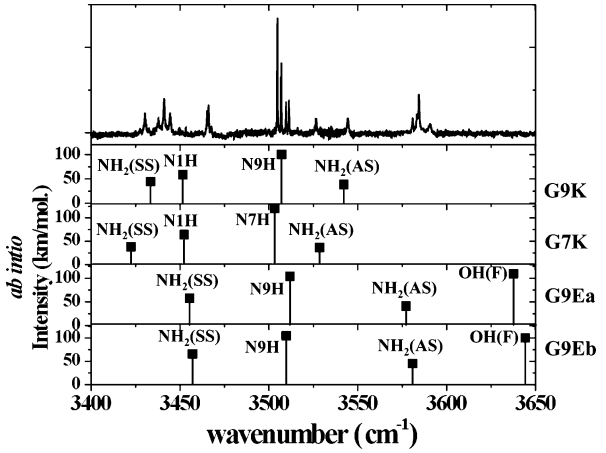

Figure 4. Survey spectrum of guanine isolated in helium droplets. The corresponding ab initio vibrational spectra for the four lowest energy tautomers of guanine are shown in separate panels below the experimental spectrum.

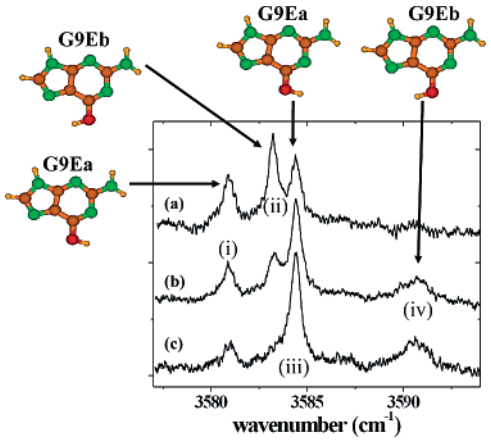

Figure 5. Expanded view of the high-frequency section (OH and NH_2 (AS)) of the guanine spectrum. Spectra a, b, and c correspond to parallel polarization, zero field, and perpendicular polarization, respectively. The assignments shown in the figure are based upon comparisons between the experimental and ab initio VTMAs and are consistent with the dipole curves presented in the Supporting Information.

these cis and trans amino-hydroxy tautomers (G9Ea and G9Eb) is afforded by the extremely low temperature and homogeneous environment provided by the helium nanodroplets. Indeed, the line widths typically observed in conventional matrices (argon, for example[21,22,61,62]) would be too broad for these four bands to be resolved.

We now shift our attention to the region corresponding to the NH_2 asymmetric stretches of the G9K and G7K isomers, which according to the scaled ab initio calculations are at 3542.2 and 3528.6 cm^{-1}, respectively. Inspection of the NH_2 (AS) region (Figure S1 in the Supporting Information) reveals that there are two bands that are in good correspondence with these ab initio frequencies and the VTMA assignments. It is interesting to note that these weak bands have not been observed in previous experimental studies of guanine.[8,14,15]

Figure 6 shows another expanded section of the guanine spectrum, in this case corresponding to the most intense bands in the spectrum near 3505 cm^{-1}. Once again, the three spectra correspond to (a) parallel, (b) zero-field, and (c) perpendicular polarization conditions. It is encouraging that both theory and experiment show four bands in this spectral region. Consider first the lowest frequency band (i), for which the experiments show strongly perpendicular behavior. According to the ab initio calculations, the lowest frequency band should be the N7H stretch of the G7K tautomer, as indicated by the vertical arrow at 3503.2 cm^{-1}. As can be seen in Table 1, the ab initio VTMA for this vibrational mode is 73°, in perfect agreement with the experimental value for the lowest frequency band in Figure 6, namely 73°. Although the experimental and calculated frequencies do not match as well as for the other three bands, the assignment is clear.

Band (ii) in Figure 6 clearly has parallel character. The scaled ab initio frequency for the G9K tautomer is in excellent agreement with experiment, and the ab initio VTMA (42°) for this N9H vibration is also in excellent agreement with the experimental value of 44°. It is evident that band (iii) is more

(61) Nowak, M. J.; Lapinski, L.; Fulara, J. *Spectrosc. Acta* **1989**, *45A*, 229−242.
(62) Szczesniak, M.; Szczepaniak, K.; Kwiatkowski, J. S.; KuBulat, K.; Person, W. B. *J. Am. Chem. Soc.* **1988**, *110*, 8319−8330.

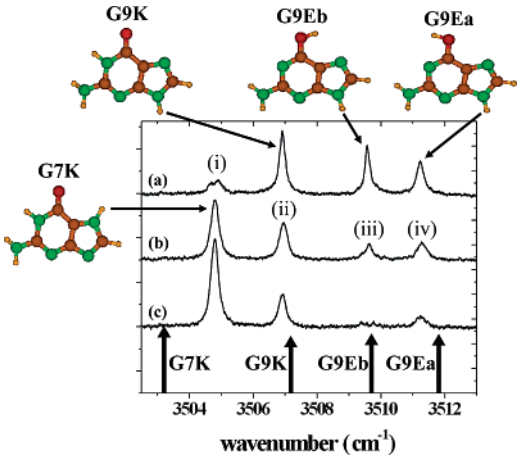

Figure 6. Assignments of the most intense bands in the guanine spectrum, based upon the VTMAs. The three spectra correspond to (a) parallel polarization, (b) zero field, and (c) perpendicular polarization. The three higher frequency bands correspond to the N9H vibrational modes of the tautomers shown, while the lowest frequency band is associated with the N7H vibrational mode of the G7K tautomer.

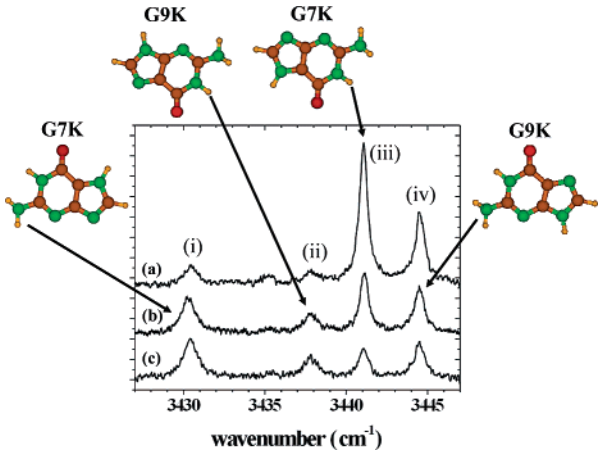

Figure 7. Low-frequency section of the experimental spectrum, recorded under (a) parallel polarization, (b) zero field, and (c) perpendicular polarization conditions. The assignments of the various vibrational bands are based upon comparisons between the experimental and calculated VTMAs.

strongly parallel in character, given that the band is strongly reduced in perpendicular polarization. The ab initio vibrational frequency suggests that this is the N9H vibration of the G9Eb tautomer. Indeed, the ab initio VTMA for this vibrational mode is 21°, in excellent agreement with the experimental value of 18°. Finally, band (iv) appears to have an intermediate VTMA between those of bands (ii) and (iii), based upon the polarization dependence of the band intensities. Assigning this band to the N9H vibration of the G9Ea tautomer, as shown in the figure, is straightforward, based on both the experimental and ab initio vibrational frequencies and the VTMAs. This is confirmed by the ab initio VTMA for this vibrational mode of 37°, in excellent agreement with the experimental value of 38°. This spectral region appears to be ideal for probing all four of the tautomers of guanine, with excellent signal-to-noise ratio.

The electric field and polarization dependence of the next two vibrational bands, near 3465 cm^{-1}, are discussed in the Supporting Information. Once again, the VTMAs for these two bands are clearly quite different, which aids in their assignment. This is particularly important in these cases, given that the ab initio vibrational frequencies for the candidate vibrational modes are in rather poor agreement with the experimental values, which are summarized in Table 1.

The final expanded spectra are shown in Figure 7, where we observe four vibrational bands. A quick tally of the modes already assigned (12) suggests that we still have four vibrational modes to identify, given that there are a total of 16, namely four vibrational modes for each of the four tautomers. Based purely on the frequency ordering of the four bands, comparisons with the ab initio frequencies would suggest that, from low to high frequency, these bands should be assigned as NH_2 (SS) of G7K, NH_2 (SS) of G9K, N1H of G9K, and N1H of the G7K tautomer. However, anticipating the assignment based on the VTMAs and dipole moment experiments (to be discussed below), we note that this assignment is good only for the NH_2 (SS) of the G7K tautomer. The observed N1H bands of the G9K and G7K tautomers are shifted farther to the red (compared to the others), so they lie between the NH_2 (SS) bands of G9K and G7K.

Band (i) is clearly perpendicular in character (experimental VTMA of 80°), consistent with the ab initio VTMA for the NH_2 (SS) of the G7K tautomer of 83°. For band (ii) the experimental VTMA is 68°, compared with the ab initio VTMA for the N1H vibration of the G9K tautomer of 80°. The difference here is a bit larger than what we have seen for the other bands, but this band is also quite weak, making the associated experimental error larger (normal experimental error being within ±5−7°).[24,56] Bands (iii) and (iv) are both clearly parallel in character, with experimental VTMAs of 20° and 40°, respectively. While the N1H stretches of the G7K and NH_2 (SS) of the G9K tautomers are both parallel bands, a comparison of the VTMAs alone does not allow us to distinguish which band belongs to which tautomer. Therefore, at this point, we will only tentatively assign bands (iii) and (iv) to G9K/NH_2 (SS) (ab initio VTMA, 31°) and G7K/N1H (ab initio VTMA, 47°), respectively. As shown below, the dipole moment measurements for these bands will confirm this assignment.

In view of the fact that some of the comparisons between the experimental and ab initio VTMAs are outside the typical differences we have come to expect from the other bands of this system, as well as from previous studies,[24,56] we were interested in developing another approach that could give an independent test of the above assignments. We discuss here an approach that takes advantage of the fact that the dipole moments for the four tautomers of guanine (see Table 1) are all quite different. As a result, the dependence of the band intensities on the magnitude of the electric field should be quite different for these tautomers. In particular, a molecule with a small dipole moment will require a large electric field for complete orientation, while much lower fields are needed to reach this saturation condition if the dipole moment is large.

Figure 8a shows a plot of the ratio of the integrated areas ($A_{\text{parallel polarization}}/A_{\text{zero field}}$) for the various vibrational bands assigned to the G9K tautomer. As indicated in Table 1, this is the tautomer with the largest ab initio dipole moment. The solid lines represent the experimental data, while the various symbols show the results calculated using the methods discussed above with the ab initio dipole moment. The agreement for all four vibrational bands is clearly excellent. In contrast to the G9K data, we present in Figure 8b the corresponding results for the G7K tautomer, which has the smallest dipole moment. In this

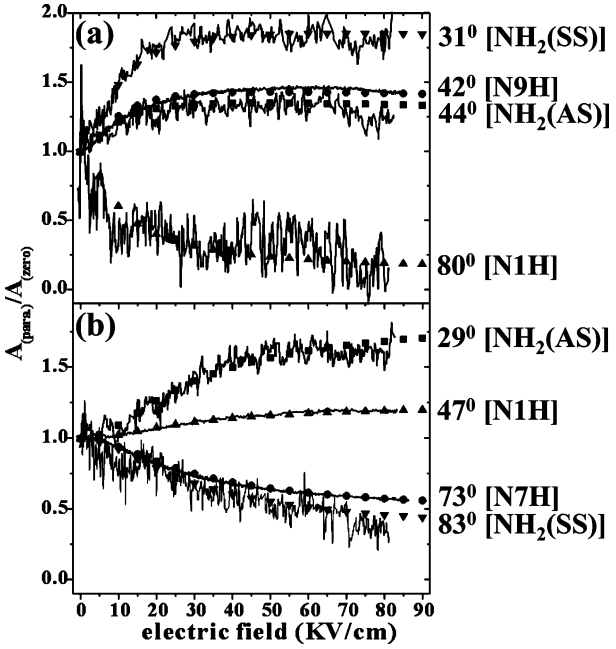

Figure 8. Plots of the electric field dependence of the ratio of the vibrational band intensities for the four vibrational modes of the (a) G9K and (b) G7K tautomers, with and without the electric field and with parallel polarization. The solid lines for the G9K and G7K tautomer show the experimental results, while the symbols correspond to the calculations based upon the ab initio dipole moment of 6.26 and 1.88 D, respectively.

case the curves are much slower to reach the saturation levels, in agreement with our expectation. Here again, the agreement between theory and experiment is quantitative for all four vibrational modes. Now, the ambiguity in the assignments of bands (iii) and (iv) in Figure 7 based on ab initio frequencies and the VTMAs is obviously resolved. Notice that, in order to get the best agreement between experiment and theory, the bands (iii) and (iv) in Figure 7 must be attributed to the N1H G7K and NH_2 (SS) G9K, respectively, confirming our previous assignments, as indicated in Figure 7. The corresponding figures for the G9Ea and G9Eb tautomers, which are clearly intermediate cases, shown in the Supporting Information, are consistent with the corresponding ab initio dipole moments. The combination of the VTMAs and these dipole curves gives us a redundancy in the assignment that is not often available. The NH_2 symmetric and N1H stretching regions clearly show that a conclusive assignment based purely on the vibrational frequency ordering cannot be obtained, given that the two bands are much closer together than the typical accuracy of ab initio calculations. Here, we show that the dipole moment curves provide unambiguous assignment of these four vibrational modes to two separate tautomers. As a result, we feel that the vibrational assignments presented here are firm. This is important, given that we now have a complete data set that can be used to make detailed comparisons with more sophisticated theories, including those which include the effects of anharmonicity.[16,63,64] In addition, we can compare our assignments to the previous gas-phase results.[14,15]

IV. Discussion

We begin this discussion by considering the discrepancy in the assignment of the N1H bands with ab initio calculations and the VTMAs. Although the separation between NH_2 (AS) and NH_2 (SS) vibrational bands of the G9K and G7K tautomers is well predicted by ab initio calculations, the calculations fail to correctly predict the ordering of the N1H and NH_2 (SS) bands of the G9K tautomer (see Table 1). This discrepancy may have several different sources, and the understanding of these could provide further insight into this system. For example, the large red shift in frequency of the N1H band of the amino-oxo tautomers (G9K and G7K) is due to a strong intramoleclar hydrogen bond. Since this interaction is sensitive to the relative orientations of the C═O, N1H, and NH_2 groups and the ring, the discrepancy with ab initio calculations may be a measure of the quality of the local geometry of these functional groups. Indeed, for this band we also observe an unusual sensitivity of the VTMAs on the basis set reflecting changes in the geometry; however, for the other bands the theoretical VTMAs show no dependence on the basis set (the typical dependence of the VTMAs on different basis sets is only $\pm 1-2°$).[25] This supports the above assumption that the VTMA discrepancy in the N1H assignment results from the failure of the 6-311++G(d,p) basis set to accurately describe the dihedral angles of the N1H groups for the G9K and G7K tautomers. In contrast, the dihedral angles of the adjacent and more remote H atoms of the NH_2 group show no change with the basis sets and are in good agreement with experiment. The dihedral angles of the N1H group in the G9K and G7K tautomers, obtained with an aug-cc-pVDZ/6-311++G(d,p) basis set, are 5°/9° and 6°/10° from the plane of the ring system, respectively. Better agreement for the N1H VTMA assignments with the aug-cc-pVDZ basis set is observed when compared to the calculations using the 6-311++G(d,p) basis set (see values in brackets in Table 1). This is likely due to the fact that the intramolecular interactions of the N1H group between the C═O and NH_2 groups are better described by the aug-cc-pVDZ basis set than by the 6-311++G(d,p) basis set. However, more theoretical work to account for the effect of anharmonicity would definitely be needed in this system. It would also be interesting to compare the ab initio vibrational frequencies, including the effects of anharmonicity, to see if the agreement with experiment is improved.

We now consider the relative integrated intensities of the various vibrational bands in the spectrum, with the goal of determining the relative populations for the four tautomers of guanine. It is helpful that we have four bands for each tautomer, giving us some redundancy in this determination. This is important, given that we have to depend on the ab initio vibrational transition moment amplitudes (see the IR intensities in Table 1) to normalize the bands relative to one another.

Considerable theoretical effort has already been devoted to the study of tautomers of neutral guanine.[21,57,65−68] It has been generally known that the G7K tautomer is most stable. Recently, Hobza and co-workers predicted that the G7K tautomer is the global minimum in both energy and Gibbs free energy, while the canonical form (G9K) is the next-lowest local minimum using the RI-MP2 method, MP2, and CCSD(T) theory with the aug-cc-pVDZ basis set.[57] They found the ordering of the relative Gibbs free energies for the four tautomers to be G7K < G9K

(63) Feynman, R. P. *Statistical Mechanics*; Perseus Books: Reading, MA, 1998.
(64) Glaesemann, K. R.; Fried, L. E. *J. Chem. Phys.* **2003**, *118*, 1596−1603.
(65) Dolgounitcheva, O.; Zakrzewski, V. G.; Ortiz, J. V. *J. Am. Chem. Soc.* **2000**, *122*, 12304−12309.
(66) Colominas, C.; Luque, F. J.; Orozco, M. *J. Am. Chem. Soc.* **1996**, *118*, 6811−6821.
(67) Leszczynski, J. *J. Phys. Chem. A* **1998**, *102*, 2357−2362.
(68) Haranczyk, M.; Gutowski, M. *J. Am. Chem. Soc.* **2005**, *127*, 699−706.

Table 2. Integrated Experimental Areas and ab Initio Relative Populations of the Guanine Tautomers

	exptl vibrational band area						
tautomer	OH[a] (F)	NH_2 (AS)	N9/7H	N1H	NH_2 (SS)	average of N9/7H and NH_2 (SS)	ab initio relative populations[b]
G9K		0.95	0.7	0.62	0.83	0.76	0.72
G7K		1	1[c]	1	1	1	1
G9Ea	1	0.77	0.34		0.36	0.35	0.44
G9Eb	0.86	0.65	0.25		0.31	0.28	0.36

[a] The free OH bands are normalized to the G9Ea tautomer. [b] Calculated as $\exp(-\Delta G/kT)$. MP2/aug-cc-pVDZ basis set was used for the free energy calculation at 620 K. [c] The intensity was compared with that of the N9H bands of the other tautomers.

< G9Ea < G9Eb, −1.8, 0.0, 0.5, and 1.8 kJ/mol, respectively. Although the calculations were done at 298 K, the ordering is consistent with our experimental observation at approximately 620 K.

On the basis of the ab initio infrared intensities and the experimental integrated intensities for all of the vibrational modes, we estimate that the experimental relative abundances of the four tautomers are 1:0.8:0.4:0.3 for G7K, G9K, G9Ea, and G9Eb tautomers, respectively. Table 2 gives a summary of the integrated experimental intensities and ab initio intensities for the four vibrational bands, normalized to the most stable G7K tautomer (except for the free OH bands, which were normalized to the G9Ea tautomer). For the N7H band of the G7K tautomer, the intensity was compared with N9H bands of the other tautomers.

Since the NH_2 (AS) bands for G9Ea and G9Eb are slightly overlapped, we averaged only the N9/7H and NH_2 (SS) bands to have a more reliable value for the relative abundances. The experimental relative abundances of the four tautomers in helium nanodroplets are in excellent agreement with those of relative free energy calculations conducted at the same temperature as used in the capture of a single molecule (ca. 620 K), as shown in Figure 2. Taking all of the data presented above together, there is no doubt that the lowest four tautomers, G7K, G9K, G9Ea, and G9Eb, are observed in helium nanodroplets.

The close correspondence between the vibrational frequencies of molecules obtained in helium droplets and those isolated in the gas-phase molecule is well known[47,69−73] and is attributed to the very weak forces between solute and solvent. However, we observe large discrepancies in the vibrational frequencies, which result in the different assignments for the guanine tautomers in our helium droplet environment relative to those obtained by de Vries and Mons using their IR−UV double-resonance approach.[8,15] A detailed comparison of the data reported by the groups of de Vries and Mons and in our work is shown in Figure 9. The vertical dotted lines are meant as a guide to compare the bands observed in the IR−UV experiments reported by (a) de Vries and (b) Mons to the IR spectrum (c) obtained from this study. A close examination shows that most of the observed bands in the IR−UV experiments do not overlap with those in this study. Figure 9 clearly shows the disagreement in the assignments of the N9H and NH_2 (AS) bands of the G9K

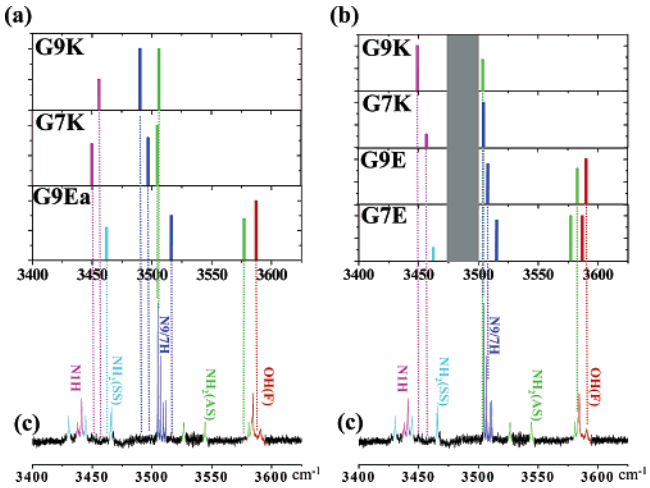

Figure 9. Direct comparisons of the guanine spectra from the three groups: (a) de Vries,[14] (b) Mons,[15] and (c) this work. The naming of each tautomer of the two different groups followed the present naming scheme. Each vibrational band is classified in different colors. The gray box in (b) is the frequency region (3470−3500 cm^{-1}) where no spectrum was taken due to the lack of IR laser power.[15] The frequencies of G7E in (b) are not compared to those of (c) due to the absence of the G7E in (c).

and G7K tautomers between the two groups, (a) and (b), mentioned in the previous papers.[14,15] Note that a direct comparison of the G7E tautomer observed in (b) cannot be made because of the absence of G7E in (a) and (c). However, the frequency patterns of G9Ea from (a) and G7E from (b) are very similar, which clearly suggests that these belong to the same molecular structure but are assigned differently. It is also interesting to note that the observation of the higher energy tautomer, G7E (see Figure 1), is questionable, because the higher energy tautomer was observed with the highest signal-to-noise ratio in the Mons experiment, but it was not observed at all in the de Vries experiments, even though the both groups used similar techniques.

The discrepancies in the assignments of specific bands for each tautomer among three groups are discussed below. First, the frequencies of the NH_2 (AS) stretch for the G9K/G7K tautomer are separated by about 50 cm^{-1}/25 cm^{-1} between the IR−UV (a and b) and this study (c). Similarly, the frequencies of the N9/7H stretch for the G9K/G7K tautomer, which was not observed by Mons due to the lack of the IR laser power in this region, are also red shifted by about 20 cm^{-1}/10 cm^{-1} between the IR−UV (a and b) and this study (c). Even if we reassigned the de Vries G9K/G7K tautomer spectra, where the NH_2 (AS) bands are assigned to the N9/7H bands, the origin of the bands at around 3490 cm^{-1} cannot be explained. Furthermore, not all the expected bands were observed in IR−UV experiments, and the specific assignments for G9K, G7K, and G9E were determined by the three (or two) observed bands out of four expected bands. Specifically, the NH_2 (SS) band for G9K and G7K in both of the IR−UV experiments is missing, even though it is observed for the G9Ea tautomer with high intensity in G9Ea (a) and moderate intensity in G7E (b). Further comparisons related to this issue can be found in the Supporting Information. As shown in Figure 9, it is clear that the discrepancy in the assignment of the infrared spectra for guanine occurs not only between the IR−UV experiments and this work, but even between the two IR−UV experiments, in which the experimental conditions are very similar. This disagreement is

(69) Hartmann, M.; Miller, R. E.; Toennies, J. P.; Vilesov, A. F. *Science* **1996**, *272*, 1631−1634.
(70) Nauta, K.; Miller, R. E. *J. Chem. Phys.* **2001**, *115*, 10254−10260.
(71) Nauta, K.; Miller, R. E. *Chem. Phys. Lett.* **2001**, *350*, 225−232.
(72) Nauta, K.; Miller, R. E. *J. Chem. Phys.* **2001**, *115*, 8384−8392.
(73) Toennies, J. P.; Vilesov, A. F. *Angew. Chem., Int. Ed.* **2004**, *43*, 2622−2648.

perhaps surprising because there has been good agreement between the gas-phase experiments and our work for the other NABs, such as adenine,[14,25,74] cytosine,[14,24,25,75] uracil,[74,76] and thymine.[74,76] The major difference between the two approaches is the method of sample preparation. While thermal evaporation methods have been used successfully for other NABs, guanine was observed to undergo decomposition before sufficient pressure was obtained.[14,15] To generate the needed vapor pressure, laser desorption methods were used in the IR−UV experiments. However, as mentioned previously, much lower vapor pressures are needed in the helium droplet experiments. Based on the definitive assignments presented in this work, thermal decomposition is apparently negligible at our oven temperatures. Since we are not performing a double resonance (selective excitation), we might also see a spectral signature of the decomposition products, which are clearly absent. It is thus possible that the discrepancy between the experiments is the result of decomposition or the presence of species other than the three and/or four lowest energy guanine tautomers in the laser desorption experiments.

V. Conclusions

This work represents the first successful IR spectroscopic study of guanine by thermal evaporation, a task made difficult by guanine's low vapor pressure. Helium nanodroplet experiments have the advantage of requiring much lower vapor pressures (10^{-6} Torr or less) than those typically used in free-jet experiments. This is important because the lower temperatures reduce the likelihood that guanine will thermally decompose. In fact, no evidence of thermal decomposition of guanine is observed at the operating temperature of our pickup cell.

In this paper we have presented a comprehensive study of guanine tautomers isolated in helium nanodroplets. When these data are combined with results from ab initio calculations, we obtain definitive assignments of all 16 observed vibrational bands for the guanine tautomers in the 3400−3650 cm^{-1} region of the spectrum. By orienting the molecules in the laboratory frame of reference, the vibrational transition moment angles (VTMAs) are measured for many of the observed vibrational bands to aid in the assignment of the specific tautomer vibrational bands. Further conclusive assignment is supported by an electric-field-dependent approach for each tautomer, taking advantage of the fact that the dipole moments for the four tautomers of guanine are all quite different. The firm assignment leads us to determine the relative populations for the four structures of guanine as 1:0.8:0.4:0.3 for the G7K, G9K, G9Ea, and G9Eb tautomers, respectively, which are in excellent agreement with those obtained from ab initio relative free energy calculations. These provide conclusive evidence that all four of the lowest energy tautomers, G7K, G9K, G9Ea, and G9Eb, are present in the helium droplets.

In this study, we have observed and identified the G9Eb tautomer that was missing in the gas-phase experiments discussed above.[14,15] The difficulty in determining the structure in several experiments could be due to its almost identical relative energy difference and the similar vibrational frequencies between the two N9H enol rotamers, G9Ea and G9Eb. We also have discussed the discrepancies in the assignments of the guanine tautomers with the previous studies.

The ab initio frequency calculations, the electric field dependence experiments (for dipole moments), and the VTMAs were used throughout this study to confirm the assignments of the various modes for the four tautomers of guanine. However, more theoretical work is needed to understand the nonplanarity of the N1H groups of the keto forms (G9K and G7K), where the VTMAs of experiment and theory show unusually large differences depending on the basis set. Nevertheless, the present study clearly shows the power of using VTMAs and dipole moments in assigning vibrational spectra and determining molecular structure, particularly when more than one isomer is present in the sample.

Acknowledgment. Support for this work from the National Science Foundation (CHE-04-46594) is gratefully acknowledged. M.Y.C. dedicates this work in memory of Roger Miller, whose death prevented him from seeing the final draft of this paper. M.Y.C. would also like to thank Prof. Tomas Baer for advice during the final stages of writing this paper.

Supporting Information Available: Energies and optimized geometries of the six guanine tautomers (G7K, G9k, G9Ea, G9Eb, G7Ea, and G7Eb), details of the VTMA analysis in the regions for the NH_2 (AS) and NH_2 (SS) bands, electric-field-dependent dipole measurements for the G9Ea and G9Eb tautomers, comparisons of the data among the three groups, and complete ref 50. This material is available free of charge via the Internet at http://pubs.acs.org.

JA060741L

(74) Colarusso, P.; Zhang, K. Q.; Guo, B.; Bernath, P. F. *Chem. Phys. Lett.* **1997**, *269*, 39−48.
(75) Nir, E.; Hünig, I.; Kleinermanns, K.; de Vries, M. S. *Phys. Chem. Chem. Phys.* **2003**, *5*, 4780−4785.
(76) Choi, M. Y.; Miller, R. E. In preparation.